AD-A065 517 PURDUE UNIV LAFAYETTE IND F/G 4/2
DISTURBED VERSUS UNDISTURBED CONDITIONS IN THE CARIBBEAN DURING--ETC(U)
MAY 78 R A TODD NSF-ATM75-10717

UNCLASSIFIED AFIT-CI-79-116T NL

| OF |
AD
A065517

END
DATE FILMED
5-79
DDC

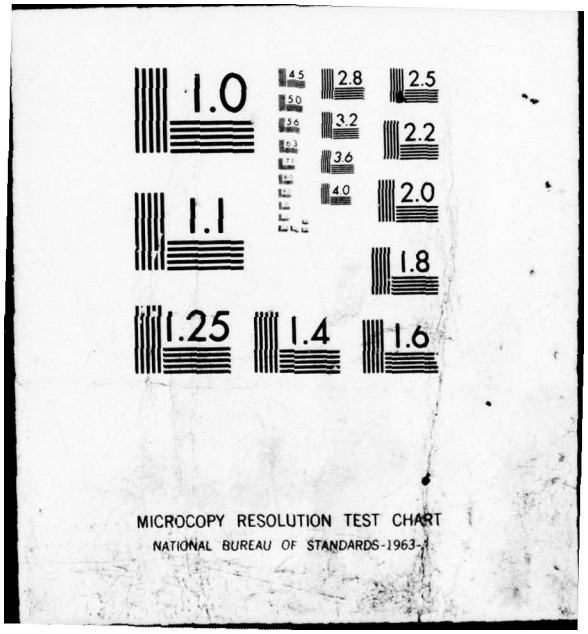
1.0
1.1
1.25
1.4
1.6
1.8
2.0
2.2
2.5
2.8
3.2
3.6
4.0
4.5
5.0
5.6
6.3
MICROCOPY RESOLUTION TEST CHART
NATIONAL BUREAU OF STANDARDS-1963-A

79-116T

LEVEL II

AD A065517

DDC FILE COPY

DISTURBED VERSUS UNDISTURBED CONDITIONS IN THE CARIBBEAN DURING THE INTENSIFICATION OF HURRICANE CARMEN (1974).

(9) Master's thesis,

A Thesis

Submitted to the Faculty

of

Purdue University

by

(15) NSF-ATM75-10717

(10) Richard Allen Todd, II

In Partial Fulfillment of the Requirements for the Degree

of

(18) AFIT/CI-79-116T (19)

Master of Science

(11) May 1978 (12) 63p.

UNCLASSIFIED

SECURITY CLASSIFICATION OF THIS PAGE *(When Data Entered)*

REPORT DOCUMENTATION PAGE		READ INSTRUCTIONS BEFORE COMPLETING FORM
1. REPORT NUMBER CI 79-116T	2. GOVT ACCESSION NO.	3. RECIPIENT'S CATALOG NUMBER
4. TITLE *(and Subtitle)* Disturbed Versus Undisturbed Conditions in the Caribbean during the Intensification of Hurricane Carmen (1974)		5. TYPE OF REPORT & PERIOD COVERED Tbesis 6. PERFORMING ORG. REPORT NUMBER
7. AUTHOR(s) Richard A. Todd, II		8. CONTRACT OR GRANT NUMBER(s)
9. PERFORMING ORGANIZATION NAME AND ADDRESS AFIT student at Purdue University		10. PROGRAM ELEMENT, PROJECT, TASK AREA & WORK UNIT NUMBERS
11. CONTROLLING OFFICE NAME AND ADDRESS AFIT/CI WPAFB OH 45433		12. REPORT DATE May 1978 13. NUMBER OF PAGES 50
14. MONITORING AGENCY NAME & ADDRESS*(if different from Controlling Office)*		15. SECURITY CLASS. *(of this report)* UNCLASSIFIED 15a. DECLASSIFICATION/DOWNGRADING SCHEDULE

16. DISTRIBUTION STATEMENT *(of this Report)*

Approved for Public Release, Distribution Unlimited

17. DISTRIBUTION STATEMENT *(of the abstract entered in Block 20, if different from Report)*

18. SUPPLEMENTARY NOTES

FEB 8 1979

JOSEPH P. HIPPS, Major, USAF
Director of Information, AFIT

19. KEY WORDS *(Continue on reverse side if necessary and identify by block number)*

20. ABSTRACT *(Continue on reverse side if necessary and identify by block number)*

DD FORM 1 JAN 73 1473 EDITION OF 1 NOV 65 IS OBSOLETE

UNCLASSIFIED

SECURITY CLASSIFICATION OF THIS PAGE *(When Data Entered)*

To Regina, Carla, and my parents
for their love and support
throughout this endeavor.

ACKNOWLEDGMENTS

My special thanks are extended to the United States Air Force for providing me the opportunity to further my education and enhance my career through this academic tour of duty.

I am sincerely grateful to Dr. Dayton G. Vincent whose guidance and constant support through successes and failures have made successful completion of this study a reality. Without his support and editorial efforts, certainly this thesis would not exist.

Sincere thanks also are extended to Drs. Christopher R. Church and Phillip J. Smith for their assistance, suggestions and critical review of this manuscript.

Special thanks go to Dr. Harold J. Edmon Jr. for his computer programming and technical assistance. My grateful appreciation goes to Ms. Marcia L. Weaks for her help in plotting and her painstaking efforts in the tedious drafting of the figures in this thesis. Sincere thanks and appreciation are extended to Miss Virginia Ewing for typing of this manuscript. This research has been sponsored in part by the Atmospheric Science Section of the National Science Foundation under Grant No. ATM75-10717 issued to Dr. Dayton G. Vincent, Purdue University.

TABLE OF CONTENTS

LIST OF TABLES

LIST OF FIGURES

ABSTRACT

Todd, Richard Allen II. M.S., Purdue University, May 1978. Disturbed Versus Undisturbed Conditions in the Caribbean During the Intensification of Hurricane Carmen (1974). Major Professor: Dayton G. Vincent.

A comparative diagnostic analysis of measured and computed properties for disturbed and undisturbed conditions in the Caribbean during Hurricane Carmen's (1974) intensification from a tropical depression just west of Guadeloupe (0000 GMT 30 August) to a major hurricane at landfall on the Yucatan Peninsula (1200 GMT 2 September) is presented. Disturbed and undisturbed regions are determined from SMS-1 infrared imagery. This satellite imagery, along with rawinsonde and surface reports taken during the Global Atmospheric Research Program's (GARP) Atlantic Tropical Experiment (GATE), represent the primary data used in this study.

Means representing eight consecutive synoptic times, 12 hours apart, beginning at 0000 GMT are presented for measured and computed quantities. Comparisons are made between conditions in disturbed and undisturbed regions, and disturbed regions are partitioned into Carmen and other disturbances. A comparison is also made between Carmen's

CONT'

CONT → values calculated in this study and those given by Vincent and Waterman (1978) for a moving volume containing Carmen.

The area of study is bounded by 30°N, 55°W, 5°N and 95°W with the northeast corner excluded due to lack of data. Quantities discussed are sea surface temperature, temperature difference, relative humidity, divergence, vertical motion, relative vorticity and kinetic energy content.

I. INTRODUCTION

In the last 10-15 years interest in tropical meteorology has significantly increased due, in part, to the advent of the meteorological satellite. The satellite not only confirmed many previously known circulation features, but also revealed many new ones. A prominent example of the latter was evidence provided by satellite photographs that a dominant scale of motion was the convectively-active cloud cluster disturbance. Cloud clusters typically contain organized convective clouds whose horizontal scale varies from 100 to 1000 km. The Global Atmospheric Research Program's (GARP) Atlantic Tropical Experiment (GATE), held from June-September 1974, had as one of its primary goals to investigate the structure and energetics of the cloud cluster disturbance.

As part of a diagnostic study of the large-scale flow during the intensification of Hurricane Carmen (1974) in the Caribbean, this study attempts to further the GATE objectives by addressing the convection problem. Infrared satellite imagery is used in conjunction with rawinsonde data to diagnose several large-scale circulation parameters associated with convective disturbances. Averages are compiled over a four-day period which is commensurate

with Carmen's life cycle over the Caribbean. The results not only show that meaningful information can be obtained from short-term averaging, but also that such averaging bridges the gap between early satellite studies which concentrated on a single satellite image and recent studies in which satellite data have been used to composite long-term means (e.g. Reed and Recker, 1971; Yanai et al, 1973; and Williams and Gray, 1973).

Among the various compositing techniques, the one used by Professor William M. Gray and his colleagues at Colorado State University (CSU) will be mentioned because it provides the most favorable points for comparison with results of this study. In the CSU technique conventional rawinsonde data are composited relative to the center of the area under observation as seen from the satellite image. Their data included two years of ESSA satellite pictures and about 12,000 rawinsonde observations. Since part of the CSU work contains long-term averages in the region near that of the present study, it is of interest to review that work. The results are summarized below and are from Ruprecht and Gray (1974, 1976a, 1976b) unless otherwise cited.

Temperature was presented in terms of the difference in virtual temperature between the clear and cloud cluster areas. Differences were generally small, between $\pm 1.4^{\circ}C$, except in the upper troposphere. The authors concluded

that relative temperature differences were insignificant. Differences in relative humidity between clear and cluster areas were 30-40% in the middle troposphere; however, below 900 mb, little difference was seen. Cloud clusters showed inflow (convergence) up to about 450 mb with a maximum at about 900 mb. Outflow (divergence) was found at higher levels with a maximum near 250 mb. Divergence values ranged from approximately $-3 \times 10^{-6} s^{-1}$ near 900 mb to $4 \times 10^{-6} s^{-1}$ near 250 mb. Vertical velocity showed a profile compatible with the divergence and had maximum upward motion of approximately 8.7×10^{-4} mb s^{-1} near 400 mb. The authors did not present similar divergence and vertical motion information for clear regions. Cloud clusters showed weak anticyclonic vorticity at all levels, while clear regions showed strong anticyclonic vorticity at all levels. Cluster vorticity maximum was about $-6 \times 10^{-6} s^{-1}$ at 100 mb while the clear area maximum was about $-16 \times 10^{-6} s^{-1}$ at 300 mb.

Low values of vertical wind shear in the troposphere have been shown to be an important parameter in the development of tropical disturbances and storms from cloud clusters; whereas, high shear zones have been cited as unfavorable (Gray, 1968). McBride (1978) investigated the vertical shear of the zonal wind in the 900 to 200 mb layer and found that strong horizontal gradients of the shear, north and south of the zero shear line, were also a significant

factor. He further defined genesis potential (GP) as $\xi_{900\ mb} - \xi_{200\ mb}$ and found that this parameter was a good indicator of cloud cluster development. He analyzed GP over a 0-6° radius of a disturbance and found values 3-4 times greater for developing tropical systems than for non-developing ones.

The various studies cited above have attempted to identify factors that might be used to distinguish developing cloud clusters from non-developing ones. This study also attempts to look at distinguishing factors; however, major differences exist between previous studies and the present one. First, the present study considers short-term averages for a particular synoptic event, as opposed to a composite of many synoptic events. Second, this study attempts to consider convectively active disturbances that are smaller in scale than the cluster size defined in the composites. Third, this study gives equal treatment to convectively inactive (undisturbed) regions. Fourth, this study also compares convective areas associated with an intensifying hurricane (Carmen, 1974) to those of other (local) disturbances. Fifth, a comparison is made between the cloud cluster identified as Carmen and the moving volume containing Carmen (Vincent and Waterman, 1978).

The goals of the present study are to: (1) determine what conditions, if any, are characteristic of convective (disturbed) and non-convective (undisturbed) activity;

(2) compare short-term results to those for the longer term, (e.g. Ruprecht and Gray, 1976a, b); (3) isolate convective activity associated with Carmen (1974) and compare meteorological conditions to those occurring in the remaining disturbed areas; (4) compare satellite derived parameters associated with Carmen to similar parameters calculated by Vincent and Waterman (1978) for a moving volume containing Carmen.

In attempting to satisfy these goals the following parameters will be considered: sea surface temperature, temperature difference (to be defined later), relative humidity, divergence, vertical motion, relative vorticity and kinetic energy content. These parameters will be compared between disturbed and undisturbed regions. Furthermore, the disturbed regions will be partitioned to isolate features attributable to Carmen so that a comparison between Carmen and other disturbed areas, as well as between Carmen and moving volume computations, can be made.

II. COMPUTATIONAL METHODS

2.1 Data Sources

The period mid-June through mid-September 1974 was a time of intense investigation of tropical meteorological phenomena. This time period corresponded to the Global Atmospheric Research Program's (GARP) Atlantic Tropical Experiment (GATE). Data collected during the GATE included conventional surface and upper air data and were supplemented by an assemblage from other observing platforms including ships, aircraft, and satellites. Surface (land and ship) and upper air reports provided the primary data sources for the present study, with geostationary satellite imagery being the guiding factor in determining how the data were composited. All these data were obtained from listings given in the GATE data catalogue in Asheville, North Carolina and include: (1) the Quick Look Data Set created from observations stored in the United Kingdom Synoptic Data Bank, (2) the National Meteorological Center GARP Level II data tapes and (3) microfilm copies of data, chart analyses and infrared SMS-1 satellite imagery maps. Additional sources of data used in this paper were the Florida State University sea surface temperature tape

(Krishnamurti et al, 1976) and the movie "14 Days of Hurricane Carmen" provided by the Goddard Institute of Space Studies, National Aeronautics and Space Administration.

Horizontal wind components and temperature were plotted and subjectively analyzed at the surface, 850, 700, 500, 400, 300, 250, 200, 150, 100 and 70 mb for each of the eight synoptic times. Relative humidity was analyzed up to its last reporting level, 300 mb. Infrared satellite brightness was used to supplement humidity reports. A value was calculated for 70 mb, based on the temperature at that level and a specific humidity of 2.3×10^{-6} (Mastenbrook, 1968), and a linear change was assumed to occur between 300 mb and 70 mb. Wind and humidity data were then extracted from the subjectively-analyzed maps at 2.5 degree latitude-longitude grid points for the region bounded by 30°N, 55°W, 5°N and 95°W, excluding a region of no data in the northeast corner, bounded by 30°N, 55°W, 25°N and 72.5°W. Analyses of gridded data, including computed values of vertical motion, were objectively analyzed by the Purdue CDC 6500 using a plotting routine obtained from NCAR. This made it possible to check for errors incurred during the data reduction process by comparing these analyses to the original hand-drawn charts. Analyses were also checked for vertical and temporal continuity and a final data set was obtained which was used in all subsequent computations.

2.2 Data Processing

Data processing began with an examination of infrared SMS-1 imagery. The original images were approximately thirty minutes apart. Although these were used for guidance and decision making, only those charts at synoptic times, twelve hours apart, were ultimately used. The study takes place from 0000 GMT 30 August 1974 to 1200 GMT 2 September 1974. The area of study, location of rawinsonde stations which provided data and Carmen's path across the Caribbean are shown in Fig. 1. Satellite images for each synoptic time are shown in Fig. 2. These images were examined to decide which areas were disturbed and undisturbed. Disturbed areas were taken to be those showing the greatest brightness, and all other areas were considered to be undisturbed. Bright areas were assumed to be representative of deep cumulus clouds and their corresponding cirrus shields. This technique is consistent with cloud-type identification practiced operationally (Anderson et al, 1974).

In order to conform to the format already available in the upper air data, disturbed and undisturbed areas, as identified from the satellite image, were reduced to a 2.5 degree latitude-longitude grid. The percentage of the area occupied by disturbed conditions in each grid square surrounding a grid point was recorded to the nearest 20%. Values of all observed and computed parameters were

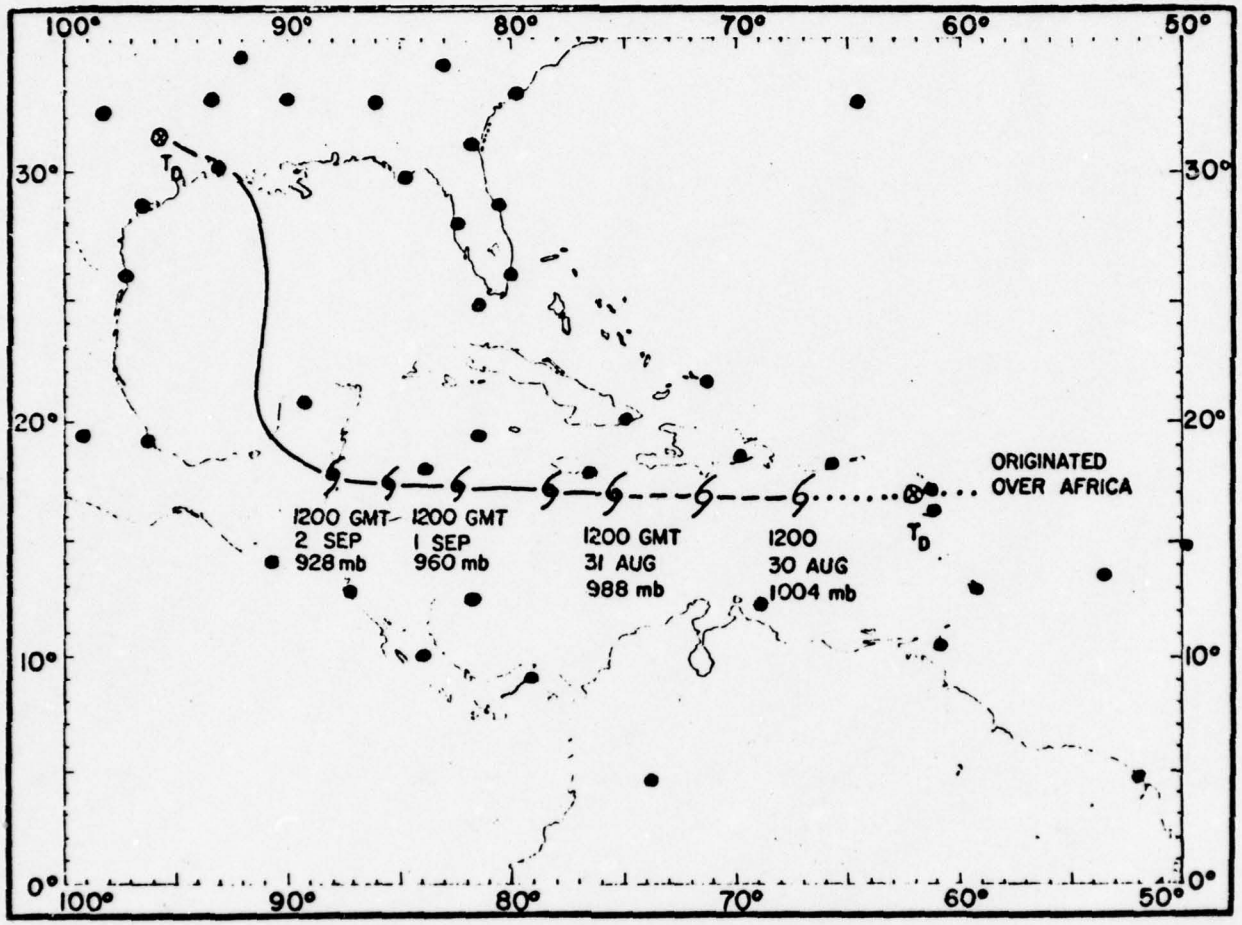

Figure 1. Area of study with storm track of Hurricane Carmen (1974) and rawinsonde stations providing synoptic data.

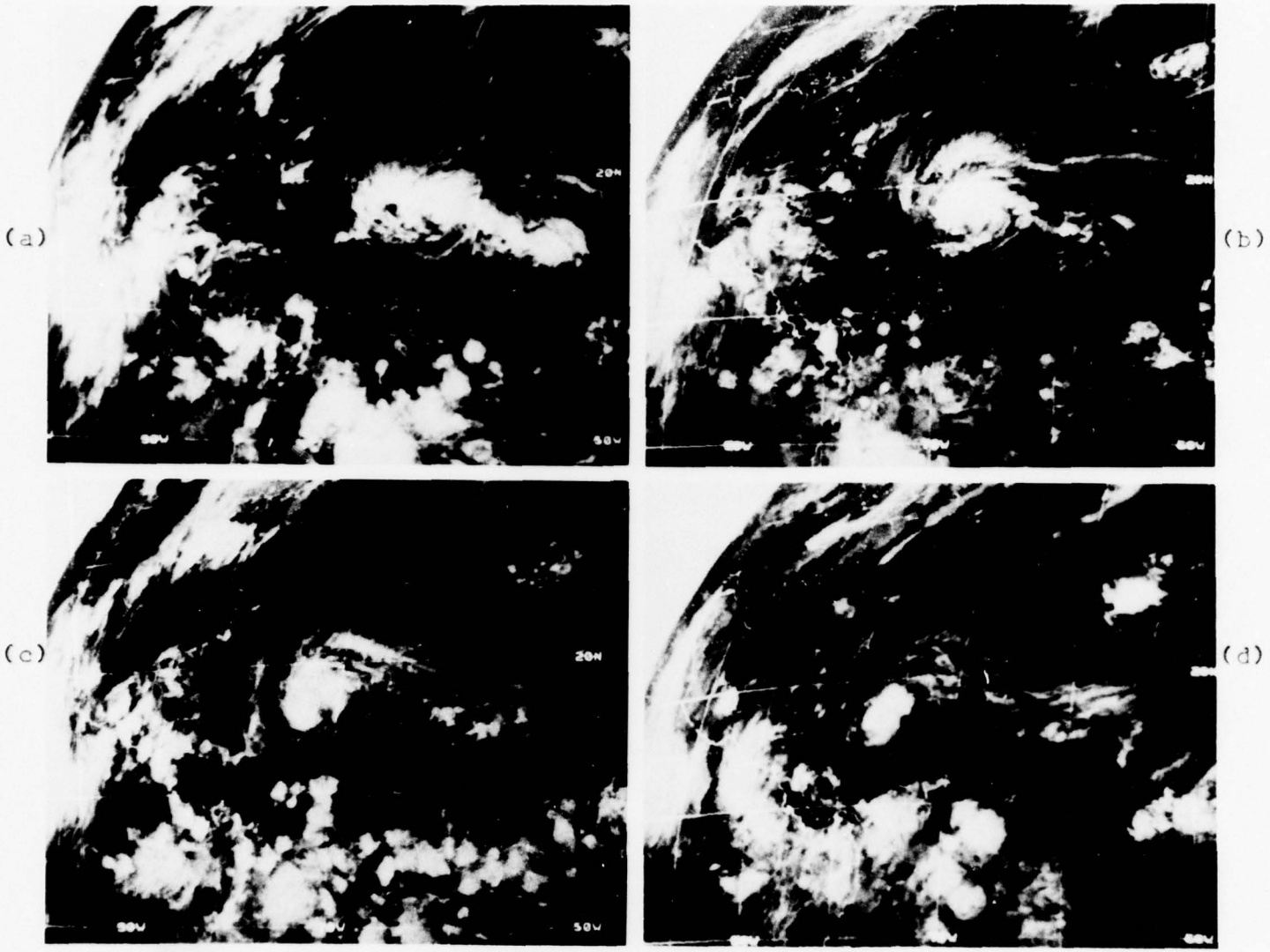

Figure 2. SMS-1 Infrared satellite imagery (a) 0000 GMT, (b) 1200 GMT 30 August 74, (c) 0000 GMT, (d) 1200 GMT 31 August 74, (e) 0000 GMT, (f) 1200 GMT 1 September 74, (g) 0000 GMT, and (h) 1200 GMT 2 September 74.

(e)

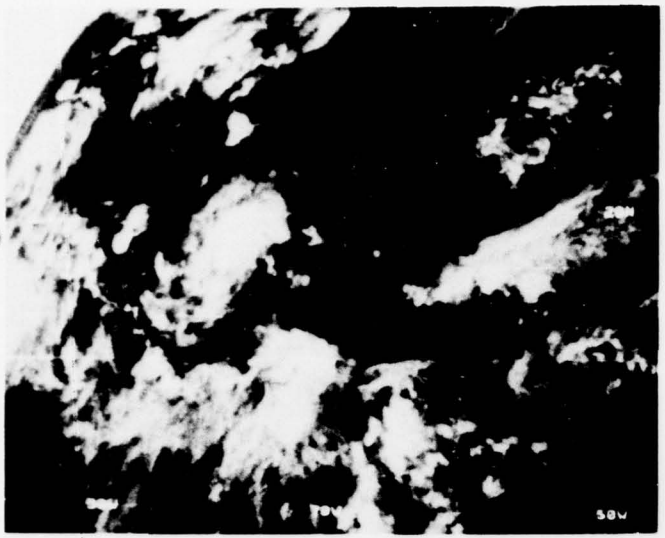

(f)

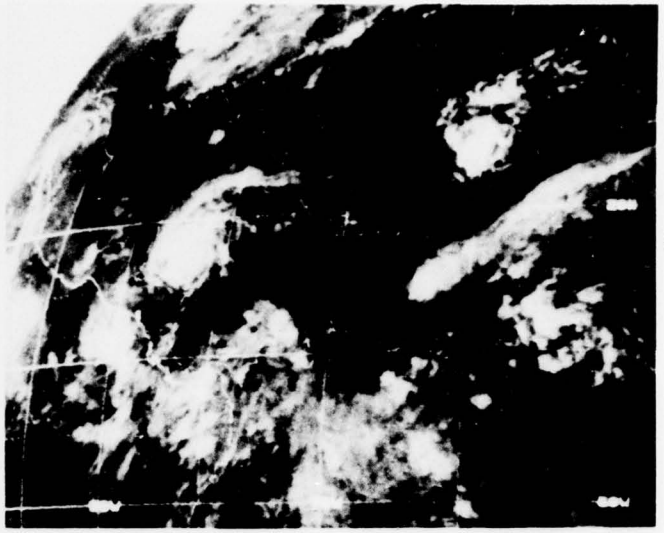

(g)

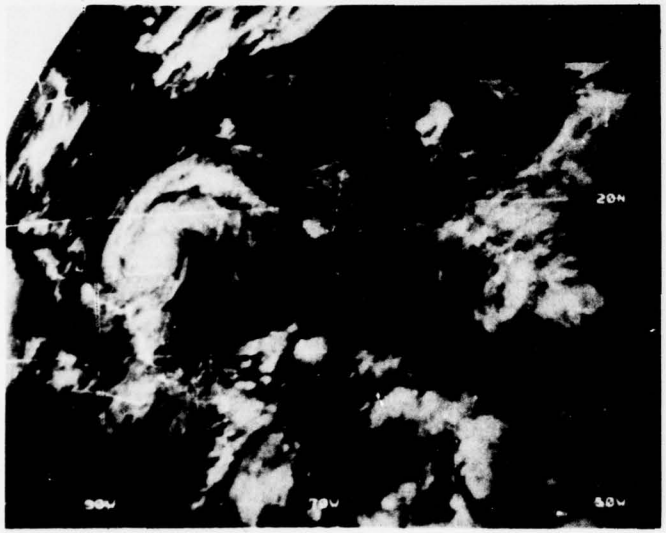

(h)

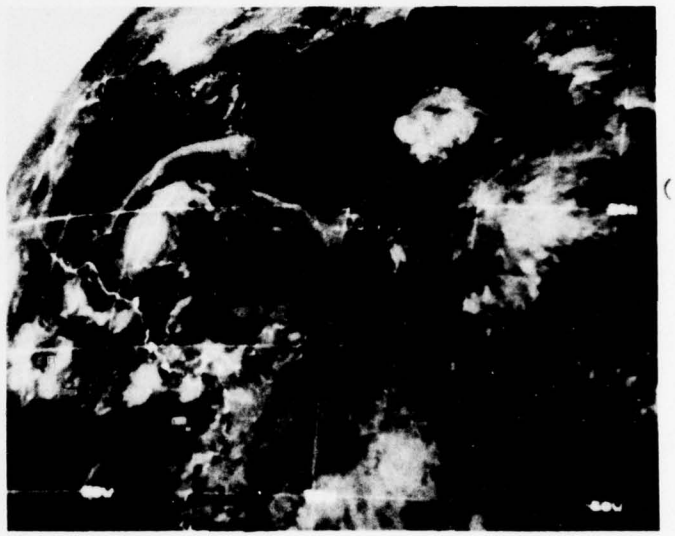

Figure 2 continued

also recorded. Weighted averages for disturbed and undisturbed values of parameters were calculated for each analysis time at the grid points shown in Fig. 3. Figure 4 shows an example of a gridded cloud map with numbers representing appropriate percentages.

For a more detailed look at disturbed areas, the satellite data were partitioned into two categories, the disturbed area associated with Carmen and the area associated with other (local) disturbances. Consequently, results were partitioned into four groups: total undisturbed, total disturbed, Carmen, and other disturbances excluding Carmen. The areas occupied by each category for each synoptic time are presented in Table 1.

2.3 Computed Quantities

All computations were performed in spherical coordinates; however, for convenience, equations are shown below in cartesian coordinates. Sea surface temperature, air temperature, and relative humidity were readily available at grid points and required no calculations. Horizontal divergence was calculated from

$$\nabla_p \cdot \vec{V} = \frac{\partial u}{\partial x} + \frac{\partial v}{\partial y} . \qquad (1)$$

Divergence values were then adjusted, using a scheme similar to that proposed by O'Brien (1970), such that the total divergence in a column of air above each grid point was zero. Vertical motions were computed by the

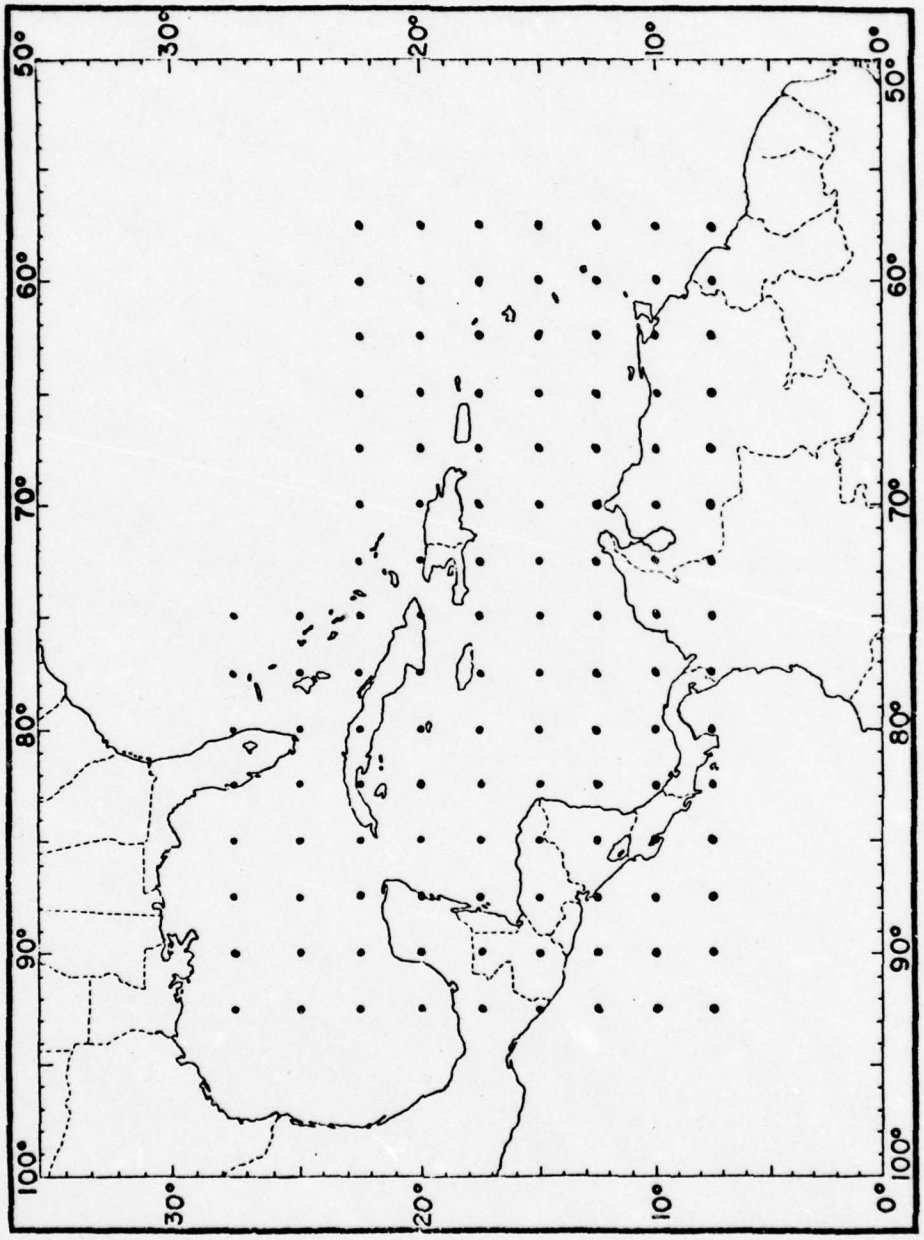

Figure 3. 2.5° latitude-longitude grid point array.

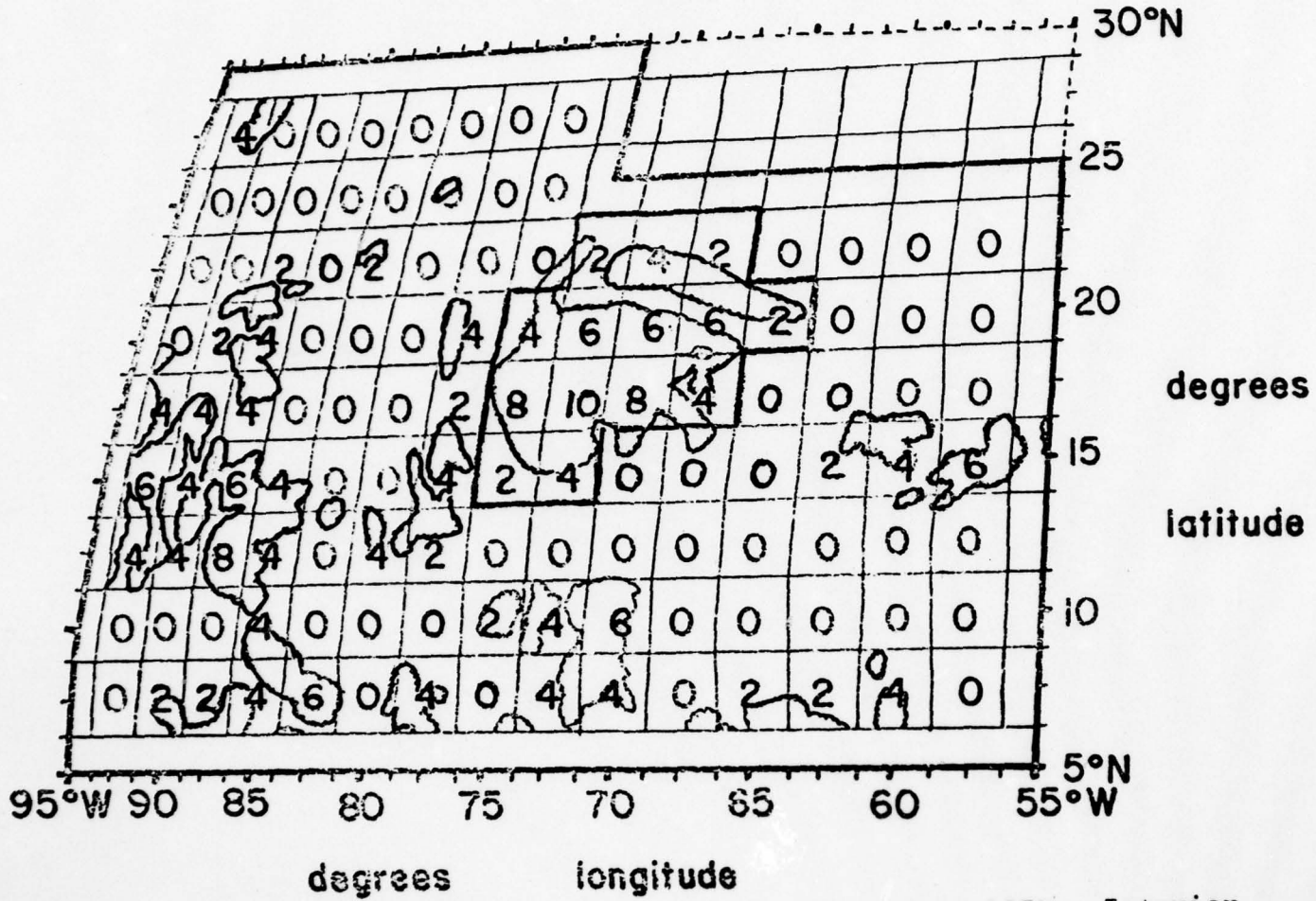

Figure 4. Gridded cloud pattern map for 0000 GMT 31 August 1974. Interior enclosed area represents the Carmen cloud cluster. Numbers indicate portion of grid square, which is disturbed, in tens of percent.

Table 1. Area and percentage of area classified as disturbed and undisturbed by analysis time. Disturbed area partitioned into Carmen and other disturbances.

Total Area: $8.9 \times 10^{12} m^2$

Analysis time	Disturbed (%)	Undisturbed (%)
1	22	78
2	16	84
3	18	82
4	14	86
5	24	76
6	16	84
7	19	81
8	10	90
Average	17	83

Analysis time	Disturbed Area ($\times 10^{12} m^2$)	Carmen (%)	Other Disturbances(%)
1	1.9	43	57
2	1.4	45	55
3	1.6	32	68
4	1.2	13	87
5	2.2	31	69
6	1.4	38	62
7	1.7	60	40
8	0.8	36	64
Average	1.5	37	63

kinematic method from (2), assuming $\omega=0$ at the surface and at 70mb,

$$\nabla_p \cdot \vec{V} = - \frac{\partial \omega}{\partial p} . \qquad (2)$$

Relative vorticity was calculated from

$$\xi = \frac{\partial v}{\partial x} - \frac{\partial u}{\partial y} . \qquad (3)$$

Finally, kinetic energy content per unit mass was computed from

$$k = \frac{u^2 + v^2}{2} . \qquad (4)$$

Each parameter was calculated for all eight analysis times and at each pressure level (or layer where appropriate). These levels were the surface 850, 700, 500, 400, 300, 250, 200, 150, 100, and 70mb. In addition to computations for the eight individual times, mean values were also derived for the entire four-day period. Moving volume profiles were obtained using data and techniques described by Waterman and Vincent (1978),but data were averaged over the entire four-day period.

III. SYNOPTIC DISCUSSION

3.1 0000 GMT 30 August 1974

At this time undisturbed conditions occupy a relatively large area (Fig. 2a and Table 1). Most noteable regions are the Gulf of Mexico, north of 20°N and the northern coast of South America. Prominent disturbed areas occur off the west coast of Florida and over, as well as south of, the Yucatan Peninsula. Several large, apparently isolated, convective cells are seen inland near the coast of South America. The dominant feature is an elongated cloud mass running east to west between about 50°N and 70°W and bounded by approximately 15°N and 20°N. This cloud cluster contains the tropical depression which becomes Hurricane Carmen. The low level (850 mb) streamline pattern (Fig. 5a) shows that easterly flow dominated throughout the region. The elongated cloud cluster's western-most portion, which contains Carmen, is located at the crest of the inverted trough. The only other significant cloud mass is in the vicinity of the Yucatan peninsula.

3.2 1200 GMT 30 August 1974

Undisturbed areas are slightly more prominent at this time than at the previous time (Fig. 2b and Table 1).

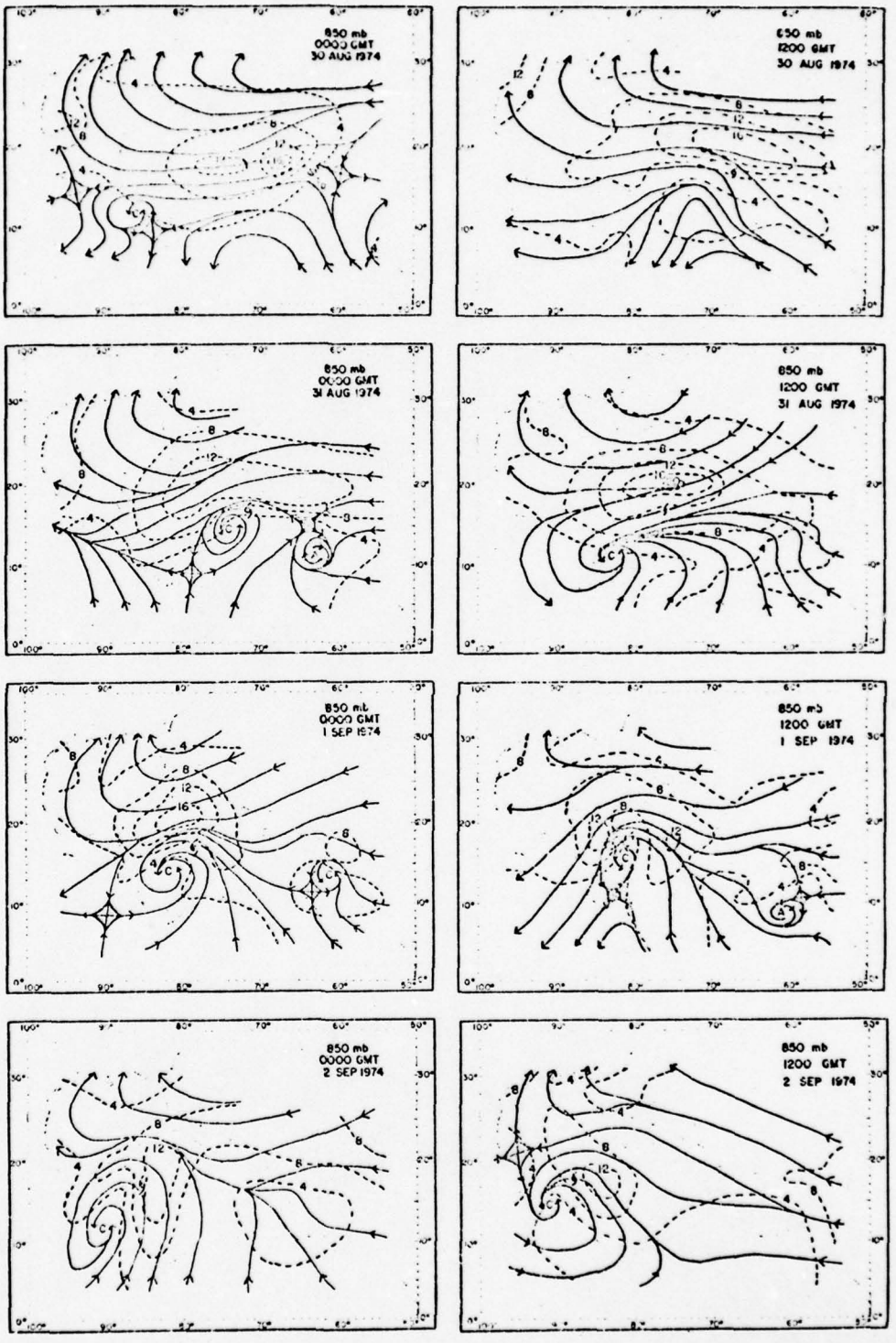

Figure 5. 850 mb streamline with isotachs in units of ms^{-1} (a) 0000 GMT, (b) 1200 GMT 30 August 74, (c) 0000 GMT, (d) 1200 GMT 31 August 74, (e) 0000 GMT, (f) 1200 GMT 1 September 74, (g) 0000 GMT, and (h) 1200 GMT 2 September 74.

Very noticeable from the cloud photographs is the decrease in the number and size of individual large convective cells and in the size of the cloud mass over the Yucatan peninsula. Furthermore, the Yucatan cloud mass now only shows a few isolated areas of disturbed conditions. The most significant change from the previous time is the development of Carmen into a tropical storm at the western end of the elongated cloud cluster. The streamline pattern shows that the wave associated with Carmen has increased in amplitude (Fig. 5b). There is also diffluence over Central America which generally corresponds with decreased convective cloudiness.

3.3 0000 GMT 31 August 1974

Again, this time shows a large proportion of undisturbed conditions (Fig. 2c, Table 1). Major disturbed regions are essentially the same as at previous times. There is a tendency for large isolated convective cells to occur over the land masses of southern Mexico, Central America, and South America. The cloud cluster containing Tropical Storm Carmen has decreased in size and shows a more distinct circulation. These cloud features are set against a background of low level easterly flow (Fig. 5c). A cyclonic center is southwest of Carmen's position but there is no apparent relation between it and the cloud pattern shown in Fig. 2c. A confluence pattern over Central America corresponds well with the large cells in that region.

3.4 1200 GMT 31 August 1974

The dominant condition over water, except for the cloud cluster containing Carmen, is undisturbed (Fig. 2d). Carmen is now at hurricane strength and has become very compact, occupying an area less than 5° in latitude and longitude. The low level streamline pattern shows the strong influence of the hurricane with flow directed toward the cyclonic center still southwest of the hurricane's position (Fig. 5d). South of 20°N, confluence is the dominant feature.

3.5 0000 GMT 1 September 1974

Disturbed conditions show an increase from the previous time with distinct isolated convective regions appearing over southern Florida and over the Yucatan peninsula (Fig. 2e, Table 1). Large disturbed areas over South America are still evident and even grow in size from the previous time. Convective cloudiness associated with Hurricane Carmen has expanded. Another cloud cluster appears between 15°N and 20°N near the eastern portion of the area of study. The streamline pattern at 850 mb continues to show a confluencepattern in the Caribbean and cyclonic center remains southwest of the hurricane's position (Fig. 5e). Confluence also corresponds well with the disturbed area over northeastern South America. Another cyclonic circulation and a small amplitude wave seem to be associated with the cloud cluster at the eastern portion of the analyzed area.

3.6 1200 GMT 1 September 1974

Major convective areas over land are nearly non-existent (Fig. 2f). The only significant disturbed areas are those associated with Hurricane Carmen and the other cloud cluster to the east, which has remained nearly stationary since the previous time. The supporting 850mb streamline pattern shows very little change in pattern except that the cyclonic circulation associated with Carmen is now located south of the hurricane (Fig. 5f). The cyclone center associated with the cluster to the east is no longer resolvable, but there is evidence of a slight wave and some corresponding confluence.

3.7 0000 GMT 2 September 1974

Small isolated convective regions are again seen over northern South America (Fig. 2g). The cloud cluster located in the eastern portion of the region appears to have decayed slightly. The western portion of the hurricane circulation is now over the Yucatan peninsula and, as a result, the areas of northern Central America and adjacent waters represent a major disturbed region. The remainder of the sea surface area is basically undisturbed. Low level streamlines (Fig. 5g) show a tendency for flow into the hurricane from the eastern Pacific instead of the Caribbean, as was the case previously.

3.8 1200 GMT 2 September 1978

Several isolated convective cells can be seen over Central America and South America; but, other than these and the disturbed area over the Yucatan peninsula associated with the hurricane, the entire region is essentially undisturbed (Fig. 2h). The 850mb streamline pattern has weakened and the only major feature remaining is the cyclonic circulation southwest of the hurricane's position (Fig. 5h).

Other synoptic discussions of hurricane Carmen can be found in Hope (1975) and Thompson and Miller (1976). The latter is based on infrared satellite photographs and discusses Carmen's complete history.

IV. RESULTS

Sea surface temperature, air temperature difference, relative humidity, divergence, vertical motion, relative vorticity, and kinetic energy content are discussed in sections 4.1 - 4.7 respectively. Section 4.8 compares Carmen's results from sections 4.1 - 4.7 to those derived for the moving volume containing Carmen, given by Vincent and Waterman (1978). Results are presented in two formats: vertical distributions (profiles) and time plots. Time plots represent the value of a particular parameter either at some designated level (or layer) or for the entire atmospheric vertical column. Each point on the time plot corresponds to one of the eight synoptic times referred to earlier. Although time plots were constructed for most quantities, many did not show any identifiable trend (e.g. diurnal, synoptic related) and, therefore, will not be discussed. For data relative to Carmen, the storm stage is also indicated. In sections 4.1 - 4.7, two sets of profiles and time plots are presented. One compares all disturbed areas to undisturbed areas and the other compares Carmen to other disturbances. The profiles in section 4.8 compare Carmen's values to those derived for the moving volume. Vertical

profiles have been area-averaged and then time-averaged over the eight analysis times.

4.1 Sea Surface Temperature

Figure 6 illustrates sea surface temperature trends. The comparison between disturbed and undisturbed traces shows lower temperatures associated with disturbed areas, presumably due to upwelling of colder water. However, it should be noted that the majority of the over-water disturbed areas were associated with Carmen throughout the study times; thus, the key features in the disturbed trace can be seen in a comparison of Carmen versus other disturbances. During its development, Carmen's sea temperatures are lower than those of other disturbed areas. As the transition is about to be made from tropical storm to hurricane, Carmen's sea temperatures become higher and remain so for the remainder of the period. Carmen's trace shows decreasing temperatures from 1200 GMT 30 August to its minimum at 1200 GMT 31 August when Carmen was first designated as a hurricane. This decrease is probably the result of upwelling of colder sea water. After 1200 GMT 31 August the sea temperature increases agree with Carmen's observed intensification even though upwelling was still occurring. Perhaps the water in the western Caribbean is warmer than that in the eastern Caribbean.

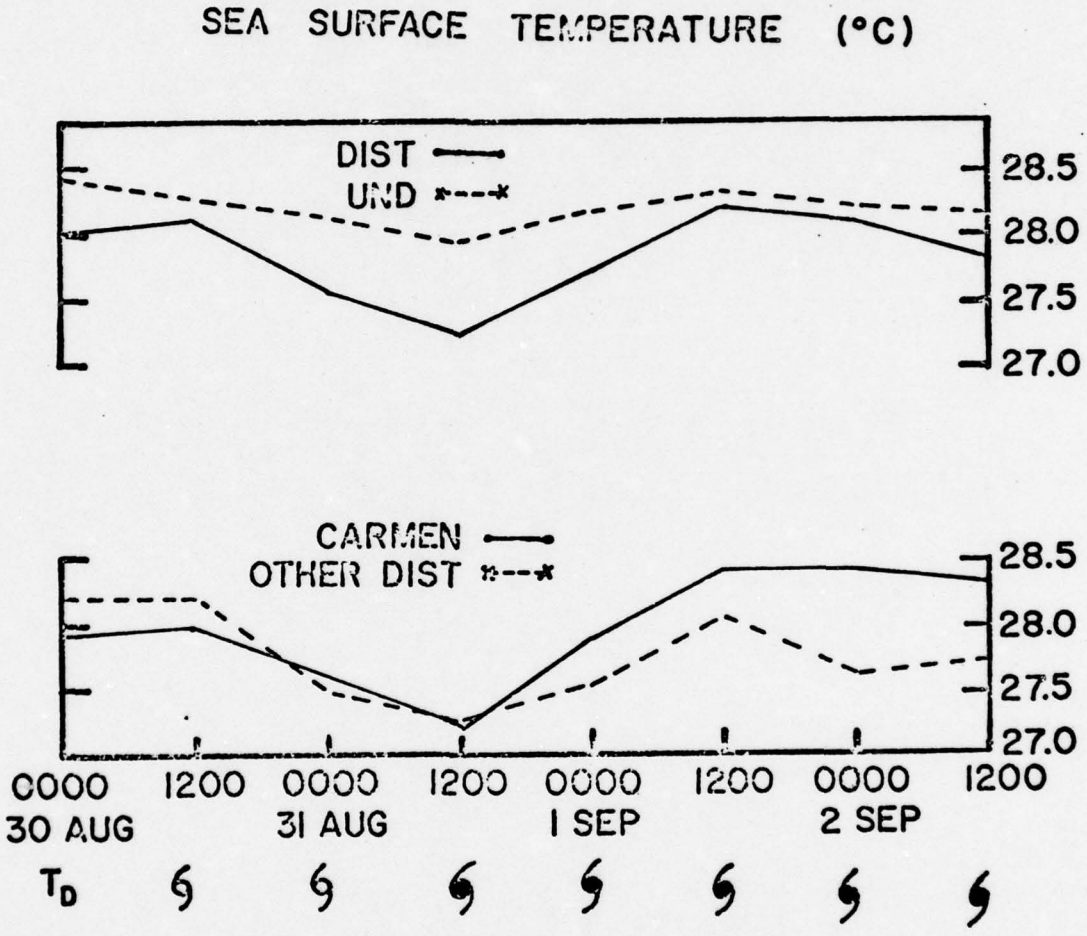

Figure 6. Temporal distribution of area-averaged sea surface temperature in units of °C.

4.2 Temperature Difference

Vertical profiles of air temperature differences (ΔT) are presented in Fig. 7. The profile on the left represents the average disturbed temperature minus the average undisturbed temperature. The significant features are the negative ΔT in the lower troposphere, positive ΔT in the mid-to-upper troposphere and return to negative values above 175 mb. The lower negative region probably illustrates the relative lack of solar radiation, lower sea surface temperatures and precipitation-induced evaporative cooling associated with disturbances. Latent heat release and/or subsidence warming on a cumulus scale within the disturbances undoubtedly accounts for the positive values of ΔT in the 600-200 mb layer. Radiative cooling above the deep cumulus convection and/or adiabatic cooling due to weak upward motion are likely explanations for the return to negative ΔT above 175 mb. The profile on the right was derived by subtracting the temperature for other disturbances from Carmen's temperature. The positive ΔT at the surface appears to be due to two factors. First, as noted previously, Carmen's sea temperatures are generally higher than those for other disturbed areas. Second, land surfaces in disturbed regions are generally colder than water surfaces. In particular, over the interior of Central America and northern South America, temperatures were sometimes as much as $14^{\circ}C$ lower than ocean temperatures.

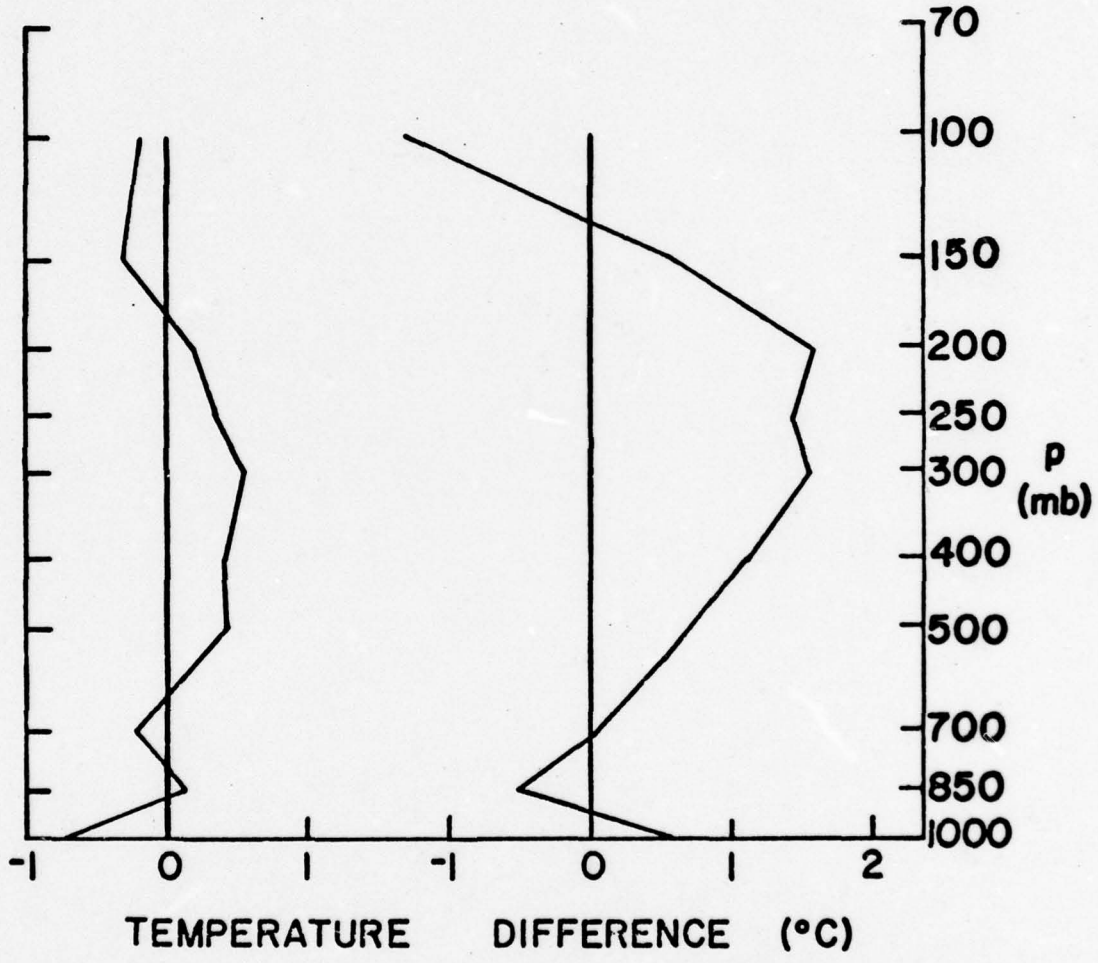

Figure 7. Vertical distribution of area-averaged temperature difference in units of ^{o}C.

Some of this difference is accounted for by elevation. Coastal regions more commonly showed temperatures 4-6°C lower than the ocean. The profile above the surface is similar to that for disturbed versus undisturbed regions, except that the positive values of ΔT are greater. This illustrates that Carmen's convective activity was more intense than that for other disturbances.

4.3 Relative Humidity

Figure 8 gives vertical profiles of relative humidity. As expected, disturbed areas show higher relative humidities than undisturbed areas. A further anticipated result is that Carmen's humidity profile shows higher values than other disturbances. An interesting point to note is the depth of moisture. Undisturbed areas only maintained $\geq$ 50% relative humidity up to about 700 mb; whereas, disturbed areas show values $\geq$ 50% up to nearly 400 mb. Comparing Carmen's profile to that for other disturbances, gives a good illustration of the depth of the atmosphere through which humid air can penetrate with intense active disturbances.

4.4 Divergence

Horizontal velocity divergence profiles are presented in Fig. 9. Undisturbed regions show a shallow layer of convergence from the surface to about 600 mb followed by weak divergence through the remaining depth of the profile. The disturbed profile shows convergence up to about 400 mb

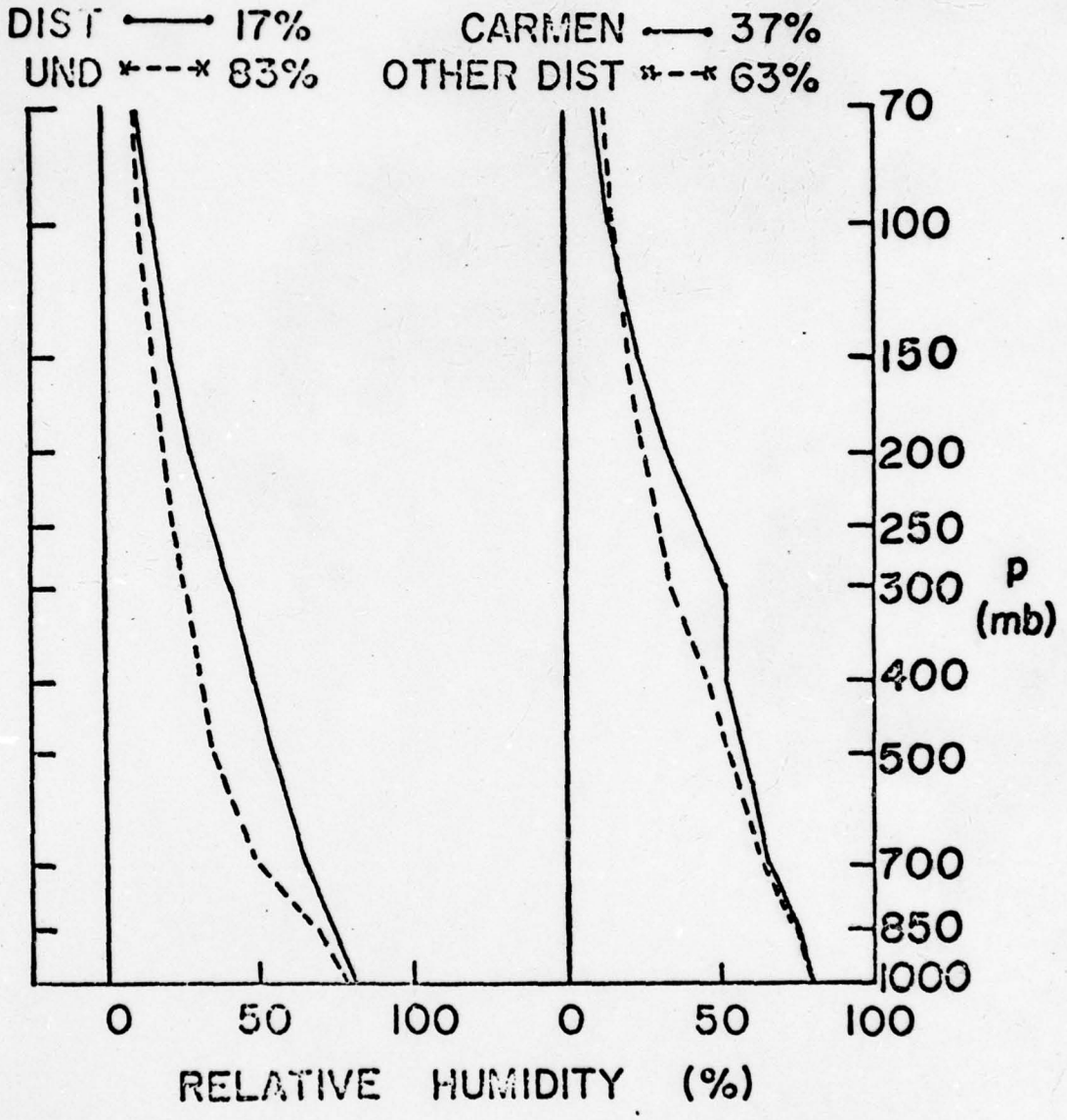

Figure 8. Vertical distribution of area-averaged relative humidity in percent.

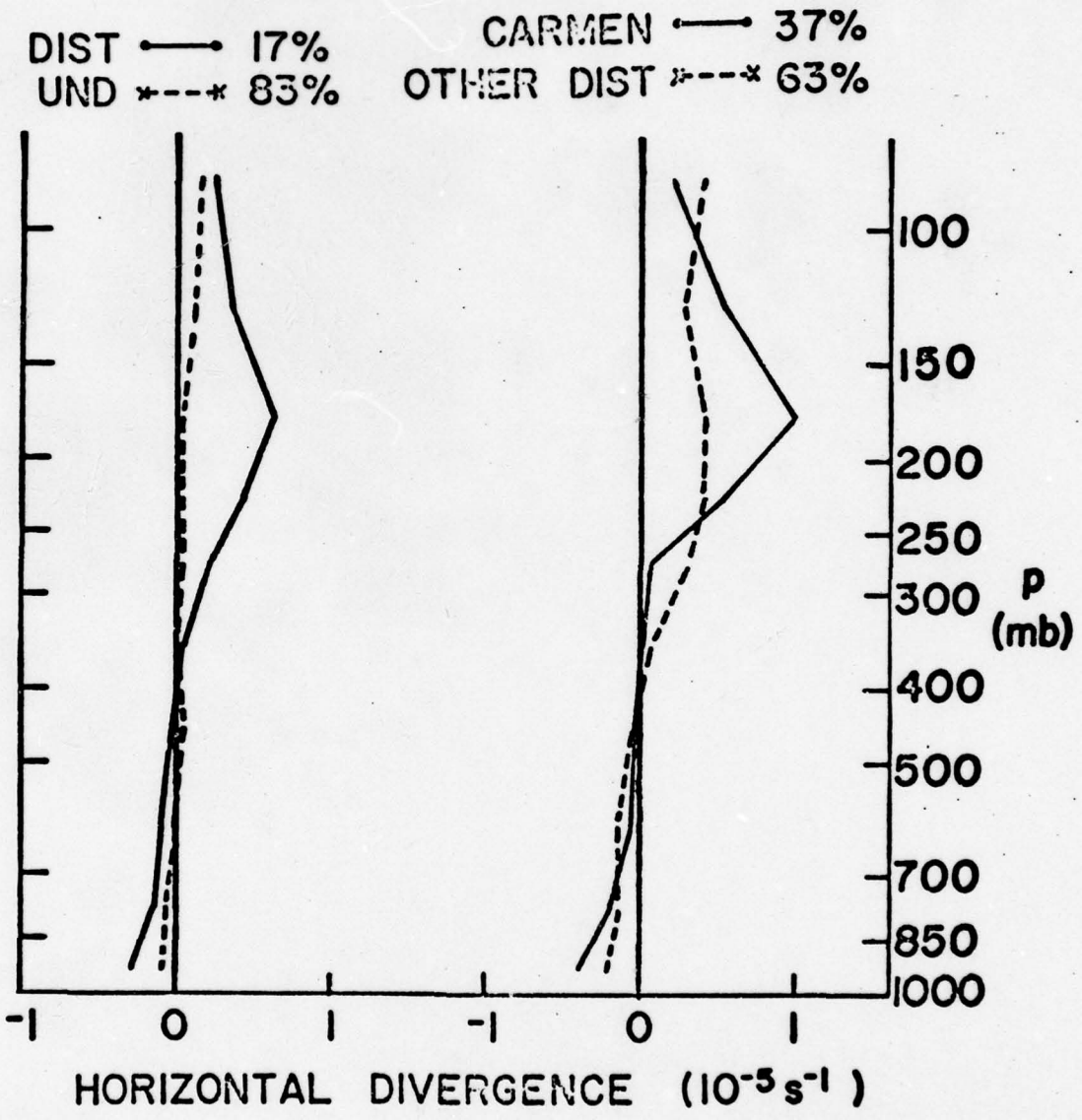

Figure 9. Same as Figure 8 except for divergence in units of $10^{-5}s^{-1}$.

with divergence above, reaching a maximum near 175 mb. When the disturbed area is partitioned for comparison between Carmen and other disturbances, both profiles show convergence from the surface up to about 400 mb, with divergence above. Of interest is the fact that Carmen's divergence shows a larger maximum than other disturbed areas, but its layer of higher values is not as deep. This profile is typical of mature hurricanes in which the upper level exhaust layer corresponds to the strong upward motion and warm core features of the system. Both of these features reach a maximum in the mid-to-upper troposphere, restricting outflow to high levels.

4.5 Vertical Motion

Vertical motion, ω, was calculated from the horizontal velocity divergence and is displayed in Fig. 10. There is upward vertical motion indicated in both disturbed and undisturbed regions, with values in disturbed regions being considerably larger. Upward motion shown for the undisturbed areas is nearly constant through the entire depth of the profile. The profile of Carmen shows higher values of upward motion than that for other disturbances. Also, maximum values extend from 500 mb to 250 mb. These results, which are similar to those given for disturbed areas in the western Pacific by Williams and Gray (1973), confirm the discussion above.

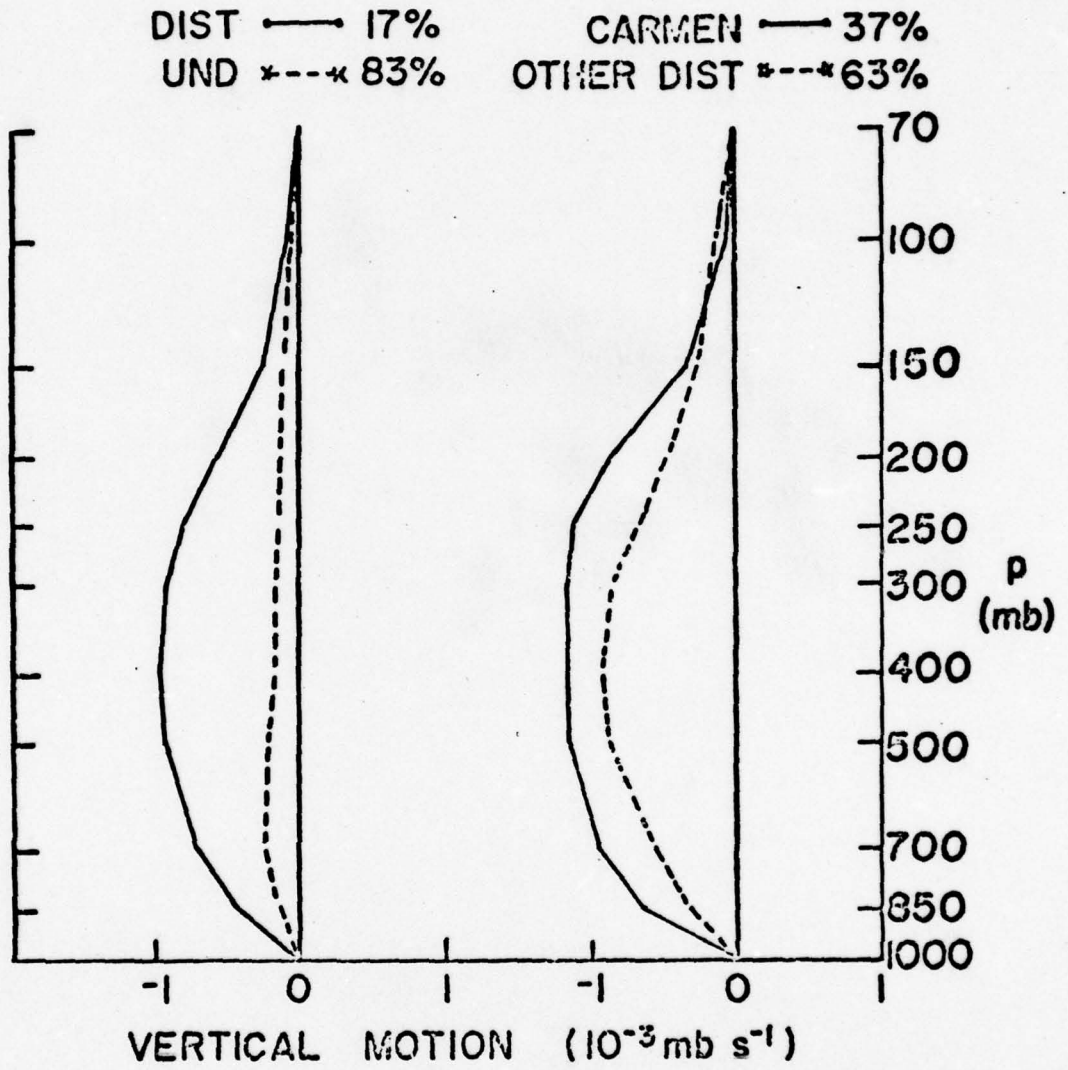

Figure 10. Same as Figure 8 except for vertical motion (dp/dt) in units of 10^{-3}mb s^{-1}.

4.6 Relative Vorticity

Figure 11 presents vertical profiles of relative vorticity. Undisturbed regions show weak anticyclonic vorticity except at the surface and upper-most levels. Maximum anticyclonic vorticity is located near 500 mb. This profile agrees with that found in clear areas in the West Indies by Ruprecht and Gray (1976a); however, their values were considerably larger. Disturbed areas show cyclonic vorticity from the surface to near 350 mb where vorticity becomes anticyclonic. Ruprecht and Gray (1976a) found that cloud clusters in the West Indies were embedded in a field of weak anticyclonic vorticity at all levels. The profile presented in the present paper resembles more closely their profile for the western Pacific cloud clusters. This finding is more realistic than it may first appear to be since the results of Ruprecht and Gray are annual means; whereas, the present results are for late summer. Furthermore, the West Indies area studied by Ruprecht and Gray was bounded approximately by latitudes 30°N and 15°N while the present area extends southward to 7.5°N (Fig. 3). In contrast, the Western Pacific area investigated by Ruprecht and Gray was bounded approximately by 15°N and the equator. Thus, the seasonal progression of climatological features (e.g., equatorial trough zone, subtropical high pressure belt) associated with disturbed and undisturbed areas suggests that the present results are not in total

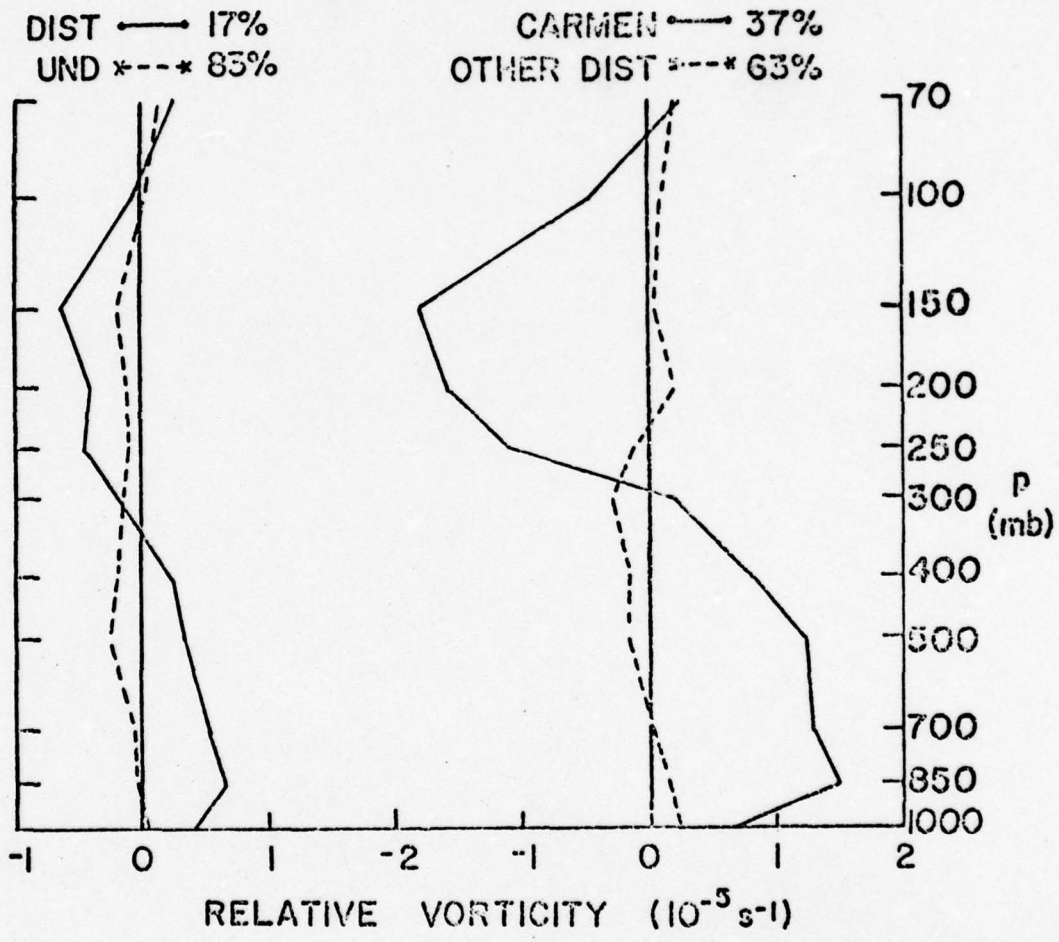

Figure 11. Same as Figure 8 except for relative vorticity in units of $10^{-5}s^{-1}$.

disagreement with those of Ruprecht and Gray. When the disturbed areas are partitioned, Carmen's profile shows strong cyclonic vorticity from the surface up to 300 mb, with anticyclonic vorticity above. Maximum cyclonic vorticity for Carmen occurred at 850 mb, while maximum anticyclonic vorticity was located at 150 mb. Other disturbances show a much shallower layer of cyclonic vorticity. The vorticity is also considerably weaker. Carmen shows a net cyclonic vorticity of about $0.6 \times 10^{-5} s^{-1}$ for the column; whereas, other disturbances show a net value of near zero. As stated in Chapter 1, McBride found that genesis potential ($\xi_{900\ mb} - \xi_{200\ mb}$) was 3-4 times greater for cloud clusters which developed into tropical storms than for those which did not. His average value of genesis potential for developing systems is $2.5 \times 10^{-5} s^{-1}$. This compares favorably to the present value of $2.8 \times 10^{-5} s^{-1}$ taken from Fig. 11 for Carmen.

4.7 Kinetic Energy Content

Figure 12 shows profiles of kinetic energy content. As anticipated, kinetic energy is greater in disturbed areas than in undisturbed areas. Also, Carmen possesses a much greater kinetic energy content than other disturbances.

Figure 13 shows time plots of vertically-integrated kinetic energy content. The most interesting feature is the comparison between Carmen and other disturbances.

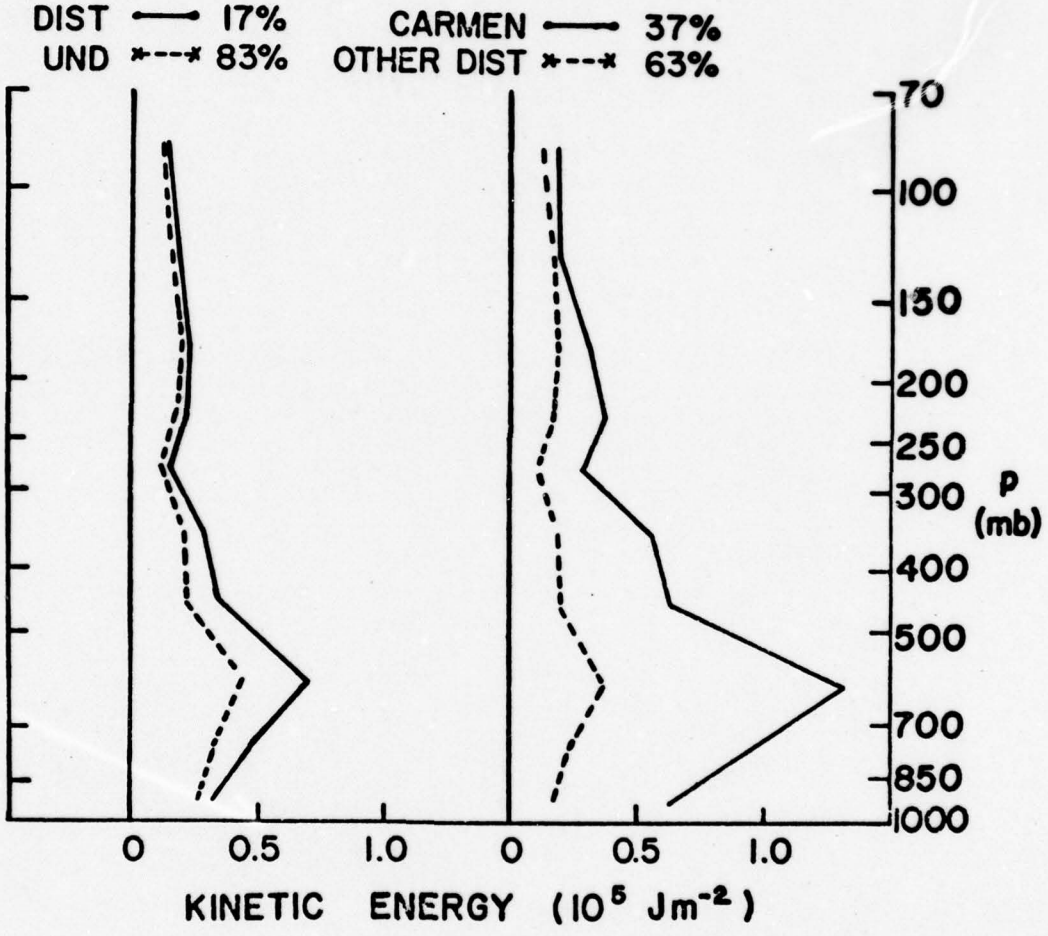

Figure 12. Same as Figure 8 except for kinetic energy content in units of $10^5 Jm^{-2}$.

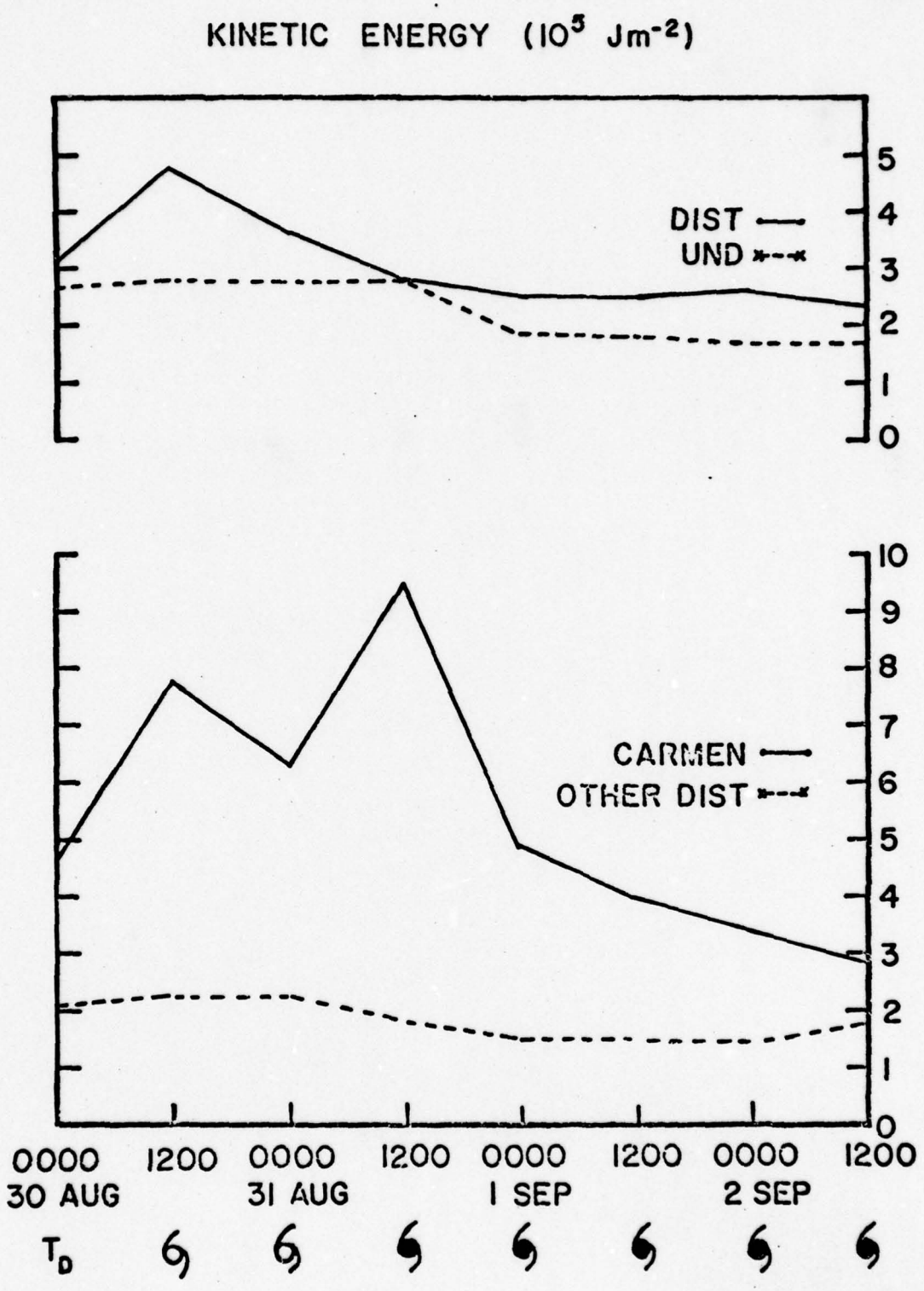

Figure 13. Same as Figure 6 except for vertical integrals of kinetic energy content in units of $10^5 Jm^{-2}$.

While other disturbances show relatively little change in kinetic energy content, Carmen shows a significant variation. Caution should be exercised, however, in interpreting the value at 1200 GMT 31 August when Carmen is first diagnosed as a hurricane. At this time its convective cloud pattern is comparatively compact, occupying less than 2% of the total area studied. At all other times, except the last, Carmen occupies 6-12% of the total area (see Table 1).

4.8 Comparison Between Carmen and Moving Volume Computations

The quantities compared are temperature difference, relative humidity, vertical motion, horizontal divergence, zonal component of the wind, relative vorticity and kinetic energy. Table 2 gives the percentage of the moving volume occupied by the disturbed area representing Carmen. Occasionally, Carmen extended beyond the boundaries of the moving volume; however, this extension never exceeded one grid distance.

The temperature difference, which was derived by subtracting the moving volume average temperature at each pressure level from Carmen's average, is shown in Fig. 14. The profile shows that the convectively-active area of Carmen is cooler in the lower troposphere and warmer in the middle and upper troposphere than the remaining area of Carmen and its environment. This implies that deep convection associated with Carmen inhibits solar insolation near the surface. When Carmen's time-averaged

Table 2. Percentage of the moving volume occupied by the disturbed area representing Carmen.

Moving Volume Area: $1.2 \times 10^{12} m^2$

Analysis Time	Carmen (%)
1	48
2	42
3	35
4	14
5	43
6	37
7	58
8	24
Average	37

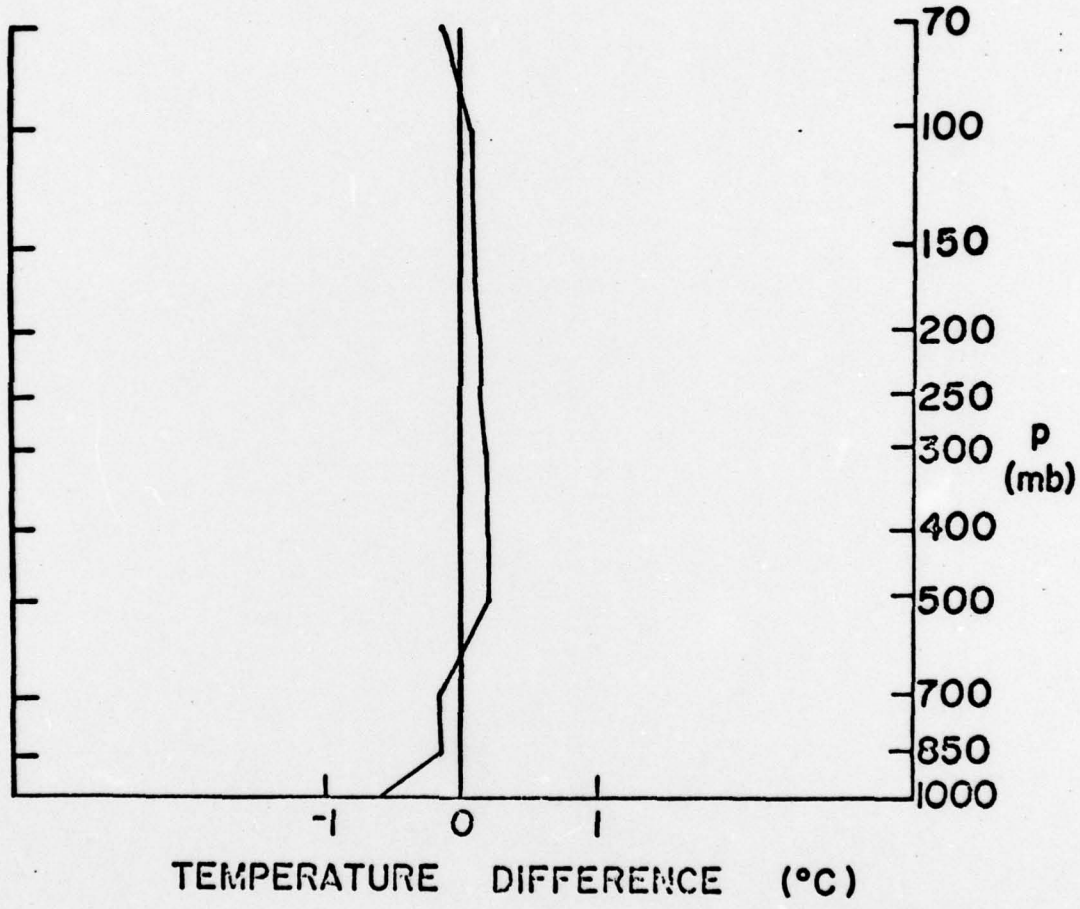

Figure 14. Vertical distribution of temperature difference between Carmen and the moving volume in units of °C.

sea surface temperature (Fig. 6) was compared to that given by Vincent and Waterman (1978) for the moving volume, the former was only about 0.1°C lower. It also appears that precipitation-induced evaporative cooling within Carmen is a contributing factor to lower temperatures at low levels. The higher temperatures in Carmen above 600 mb are most likely due to latent heating.

Figure 15 shows relative humidity profiles for Carmen and the moving volume, as well as the difference between the two profiles. Note that Carmen's values exceed those for the moving volume in the 600-250 mb by at least 5%.

Figure 16 shows comparative profiles of vertical motion, horizontal divergence, zonal component of the wind and relative vorticity. Carmen's values are similar to those for the moving volume, but slightly greater in magnitude. The smaller values for the moving volume are probably due to its larger area which includes more of the storm's environment.

Figure 17 shows profiles of kinetic energy content. Profiles are almost identical with Carmen's values being slightly greater at all levels. The vertically-integrated value for Carmen is about 20% greater than that for the moving volume.

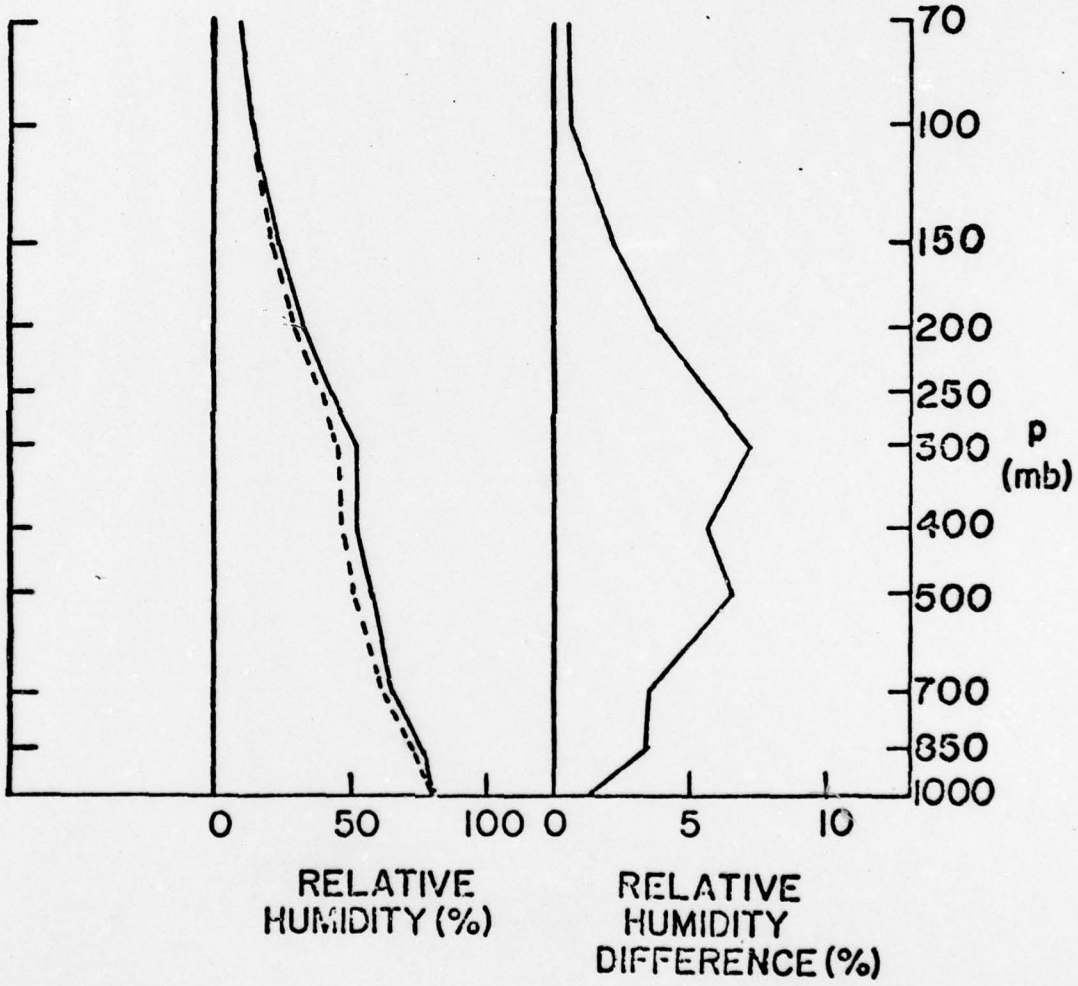

Figure 15. Vertical distribution of area-averaged relative humidity (left) for Carmen (solid line) and the moving volume (dashed line), relative humidity difference between Carmen and the moving volume (right). Humidity given in percent.

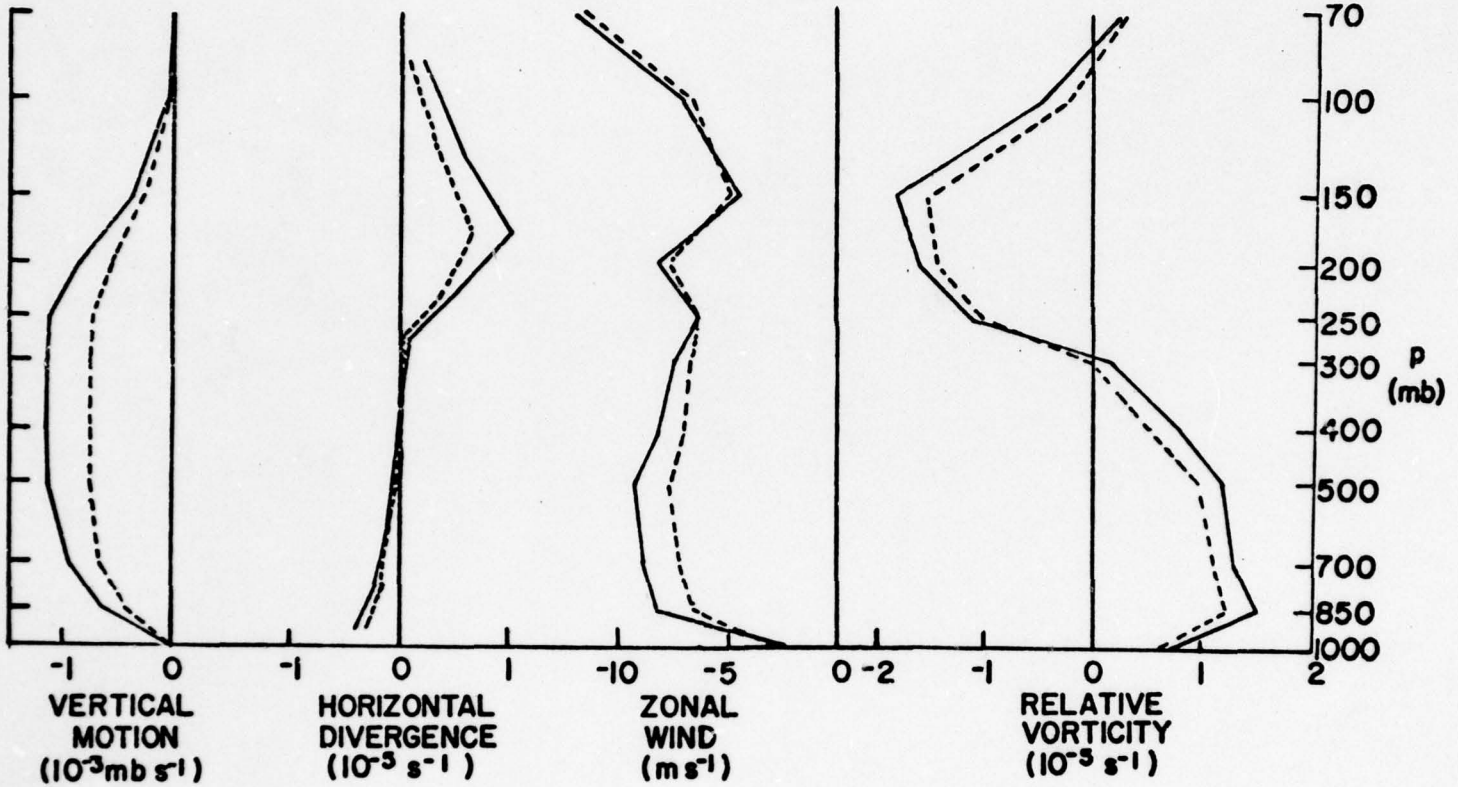

Figure 16. Vertical distribution of area-averaged kinematic quantities for Carmen (solid line) and the moving volume (dashed line) for vertical motion (dp/dt) in units of 10^{-5}mb s^{-1}, divergence in units of $10^{-5}s^{-1}$, zonal wind component in units of ms^{-1}, and relative vorticity in units of $10^{-5}s^{-1}$,

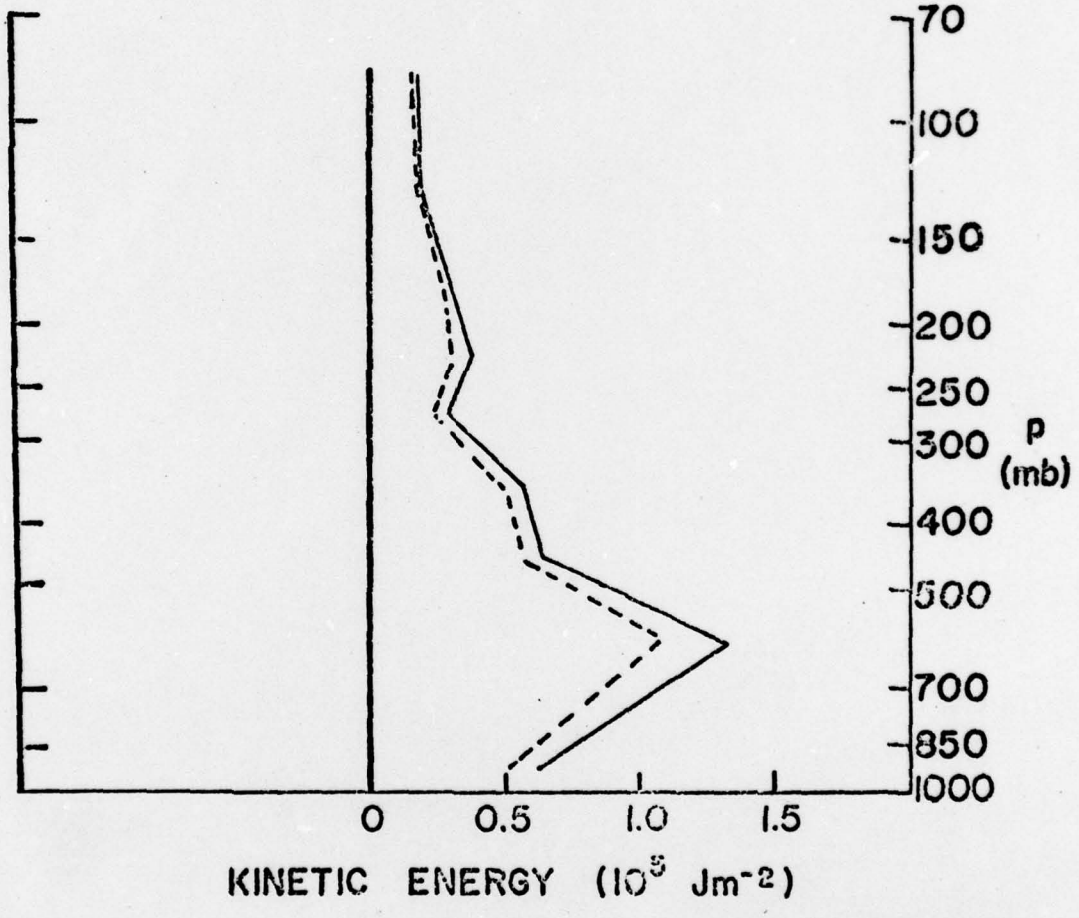

Figure 17. Same as Figure 16 except for kinetic energy content in units of 10^5 Jm^{-2}.

V. CONCLUSIONS

In this study a diagnostic comparison has been made between disturbed and undisturbed conditions in the Caribbean area during the intensification of Hurricane Carmen. Disturbed and undisturbed areas were identified using SMS-1 infrared imagery. The period of study was 0000 GMT 30 August 1974 through 1200 GMT 2 September 1974 and was coincident with Carmen's development from a tropical depression to a major hurricane. The period of study also fell within the Global Atmospheric Research Program's (GARP) Atlantic Tropical Experiment (GATE) which took place from mid-June to mid-September 1974.

Satellite pictures have been used in this study to partition results into those applicable to disturbed and undisturbed areas. Disturbed areas have been further partitioned into Carmen and other disturbances. Rawinsonde data were used to determine the distribution of several observed and computed parameters in each of these four groups.

One of the goals of this study was to ascertain if meaningful information could be gleaned from short-term averages for a single case study. Previous studies have

relied on long-term composited means. In general, it was found that the present short-term means did yield meaningful results and it is suggested that the technique used in this study is worthy of further consideration.

The main conclusions of this study are summarized below. First, lower sea surface temperatures were found to be associated with disturbed areas. Second, except in the subcloud layer where there was a lack of solar insolation and evaporative cooling occurred, and at cloud top heights where adiabatic and radiative cooling took place, disturbed areas were warmer than undisturbed areas. Third, relative humidities $\geq$ 50% were found to extend over a greater depth in disturbed areas. Fourth, low level convergence and upper level divergence were found in both disturbed areas and undisturbed areas; however, undisturbed values were extremely small. Carmen's low level convergence and upper level divergence were greater than those found in other disturbances and its maximum divergence was restricted to a narrower layer. This feature is common of most mature hurricanes. Fifth, both disturbed and undisturbed areas exhibited upward vertical motion; however, undisturbed values were small. The strongest upward motion was found in Carmen. Sixth, relative vorticity profiles showed that disturbances were characterized by low level cyclonic vorticity with upper level anticyclonic vorticity. The depth of the low level cyclonic vorticity was greater for Carmen than for other disturbances.

Undisturbed areas existed in a field of anticyclonic vorticity through nearly the entire depth of the column. Seventh, very little difference existed between the kinetic energy of disturbances other than Carmen and undisturbed areas; however, Carmen's kinetic energy was considerably greater than that for other disturbances.

Comparisons made between the active cloud portion of Carmen and the larger moving volume containing Carmen and its environment (Vincent and Waterman, 1978), showed remarkable similarity in area-averaged vertical profiles. The present values were generally a little greater, presumably due to the larger area over which quantities were averaged in the Vincent and Waterman results.

Though the technique applied in this study was generally successful, it is conceivable that the identification of disturbed areas could be improved if special types of data were available. For example, radar echoes received from the Planned-Position Indicator (PPI) and Range-Height Indicator (RHI) could serve as a cross reference to insure that only true deep convection was identified from the satellite imagery. In addition, infrared image enhancement of satellite irradiance or derived temperatures, could be used with the assumption of some discriminant value as an indicator of deep convection.

REFERENCES

REFERENCES

Anderson, R.K., J.P. Ashman, F.E. Bittner, G.R. Farr, E.W. Ferguson, V.J. Oliver, and A.H. Smith, 1974: Application of meteorological satellite data in analysis and forecasting. ESSA Technical Report NESC 51. National Oceanic and Atmospheric Administration, 342 pp.

Gray, W.M., 1968: Global view of the origin of tropical disturbances and storms. Mon. Wea. Rev., 96, 669-700.

Hope, J.R., 1975: Atlantic hurricane season of 1974. Mon. Wea. Rev., 103, 285-293.

Krishnamurti, T.N., V. Wong, H.L. Pan, G. VanDam and D. McClellan, 1976: Sea surface temperatures for GATE. Report 76-3, Dept. of Meteorology, Florida State University, 268 pp.

Mastenbrook, H.J., 1968: Water vapor distribution in the stratosphere and high troposphere. J. Atmos. Sci., 25, 299-311.

McBride, J.L., 1978: Observational analysis of the differences between developing and non-developing tropical disturbances. 11th Technical Conference on Tropical Meteorology and Hurricanes. Miami Florida, December, 1977, American Meteorological Society, Boston, Mass., 260-267.

O'Brien, J.J., 1970: Alternative solutions to the classical vertical velocity problem. J. Appl. Meteor., 9, 197-203.

Reed, R.J. and E.E. Recker, 1971: Structure and properties of synoptic-scale wave disturbances in the equatorial western Pacific. J. Atmos. Sci., 28, 1117-1133.

Ruprecht, E. and W.M. Gray, 1974: Analysis of satellite-observed tropical cloud clusters. Atmospheric Science Paper No. 219, Dept of Atmospheric Science, Colorado State University, Fort Collins, Colorado, 91 pp.

_____, 1976a: Analysis of satellite-observed tropical cloud clusters. I. Wind and dynamic fields. Tellus, XXVIII, 391-413.

_____, 1976b: Analysis of satellite-observed tropical cloud clusters. II Thermal, moisture, and precipitation. Tellus, XXVIII, 414-425.

Thompson, O.E., and J. Miller, 1976: Hurricane Carmen: August-September 1974- Development of a wave in the ITCZ. Mon. Wea. Rev., 104, 1194-1199.

Vincent, D.G. and R.G. Waterman, 1978: Large-scale atmospheric conditions during the intensification of Hurricane Carmen (1974). I. Temperature, moisture, and kinematics. (submitted to Monthly Weather Review).

Waterman, R.G. and D.G. Vincent, 1978: Large-scale kinematic and moisture analysis during the intensification of Hurricane Carmen (1974). 11th Technical Conference on Tropical Meteorology and Hurricanes. Miami, Florida, December, 1977, American Meteorological Society, Boston, Mass., 608-615.

Williams, K.T. and W.M. Gray, 1973: Statistical analysis of satellite-observed trade wind cloud clusters in the western north Pacific. Tellus, XXV, 313-336.

Yanai, M., S. Ebensen and J. Chu, 1973: Determination of bulk properties of tropical cloud clusters from large-scale heat and moisture budgets. J. Atmos. Sci., 30, 611-627.

APPENDIX

APPENDIX

p	pressure
t	time
d	total derivative operator
∂	partial derivative operator
∇_p	del operator on an isobaric surface
$\vec{V}$	horizontal wind vector on an isobaric surface
u	zonal component of velocity
v	meridional component of velocity
ω	vertical motion (dp/dt)
ξ	relative vorticity
x	zonal direction
y	meridional direction
k	kinetic energy content